forests

MDPI

Article

Aboveground Carbon Stocks across a Hydrological Gradient: Ghost Forests to Non-Tidal Freshwater Forested Wetlands

Christopher J. Shipway [1,*], Jamie A. Duberstein [1], William H. Conner [1], Ken W. Krauss [2], Gregory B. Noe [3] and Stefanie L. Whitmire [1]

[1] Baruch Institute of Coastal Ecology and Forest Science, Clemson University, Georgetown, SC 29440, USA; jdubers@clemson.edu (J.A.D.); wconner@clemson.edu (W.H.C.); whitmi6@clemson.edu (S.L.W.)
[2] U.S. Geological Survey, Wetland and Aquatic Research Center, Lafayette, LA 70506, USA; kraussk@usgs.gov
[3] U.S. Geological Survey, Florence Bascom Geoscience Center, Reston, VA 20192, USA; gnoe@usgs.gov
* Correspondence: cjsshipway@gmail.com

Abstract: Upper estuarine forested wetlands (UEFWs) play an important role in the sequestration of atmospheric carbon (C), which is facilitated by their position at the boundary of terrestrial and maritime environments but threatened by sea level rise. This study assessed the change in aboveground C stocks along the estuarine–riverine hydrogeomorphic gradient spanning salt-impacted freshwater tidal forested wetlands to freshwater forested wetlands in seasonally tidal and nontidal landscape positions. Standing stocks of C in forested wetlands were measured along two major coastal river systems, the Winyah Bay in South Carolina and the Savannah River in Georgia (USA), replicating and expanding a previous study to allow the assessment of change over time. Aboveground C stocks on these systems averaged 172.9 Mg C ha^{-1}, comparable to those found in UEFWs across the globe and distinct from the terrestrial forested ecosystems they are often considered to be a part of during large-scale C inventory efforts. Groundwater salinity conditions as low as 1.3 ppt were observed in conjunction with losses of aboveground C. When viewed in context alongside expected sea level rise and corresponding saltwater intrusion estimates, these data suggest a marked decrease in aboveground C stocks in forested wetlands situated in and around tidal estuaries.

Keywords: upper estuarine forested wetlands; tidal freshwater forested wetlands; blue carbon; ecosystem carbon; climate change; salinity intrusion

Citation: Shipway, C.J.; Duberstein, J.A.; Conner, W.H.; Krauss, K.W.; Noe, G.B.; Whitmire, S.L. Aboveground Carbon Stocks across a Hydrological Gradient: Ghost Forests to Non-Tidal Freshwater Forested Wetlands. *Forests* **2024**, *15*, 1502. https://doi.org/10.3390/f15091502

Academic Editor: Mark E. Harmon

Received: 28 June 2024
Revised: 1 August 2024
Accepted: 19 August 2024
Published: 28 August 2024

1. Introduction

Blue carbon ecosystems such as seagrass beds, salt marshes, and mangroves have rates of carbon (C) burial (138–218 g C m^2 yr^{-1}) that greatly outpace those of terrestrial forests (4–5 g C m^2 yr^{-1}) [1], distinguishing these habitats as being of critical importance in understanding the global C cycle and driving extensive scientific investigation on their potential to reduce atmospheric C concentrations [1–8]. While the precise definition of a blue C ecosystem is inherently qualitative and subject to ongoing debate [9,10], exceptionally high C sequestration potential remains a consistent descriptor. Only recently included in global blue C inventories, Upper Estuarine Forested Wetlands (UEFWs), also referred to as tidal freshwater forested wetlands (TFFWs), are found worldwide spanning the estuarine gradient between traditional freshwater nontidal wetlands and lower elevation blue C ecosystems [10–13]. This estuarine gradient is composed of contributory hydrogeomorphic transitions in elevation, salinity, and tidal influence [10] that are typical of the riverine–estuarine boundary. The position of UEFWs along this complex interface of terrestrial and maritime environments enables them to play critical roles in local ecology [2,5,14,15] and coastal biogeochemistry (i.e., sediment and nutrient retention [11]), while exhibiting large [16] but often imprecisely quantified [17] aboveground standing C stocks and burial rates [1,14,18]. These diverse UEFWs are subjected to a complex set of environmental drivers including the presence of freshwater tidal flushing at their landward distributional

limit and salinity pulsing more seaward [15,19,20], creating a rarely described series of drivers to the ecology of any functionally freshwater ecosystem. Because UEFWs are not identified by a specific vegetation type, they are difficult to map, often seen as simply transitional, and therefore overlooked [21]. However, UEFWs occupy thousands of hectares in the Southeastern US alone [22] and are present in many other countries (e.g., [13,23]).

To quantify C stocks in UEFWs along two Southeastern US river systems, our study sites span the estuarine gradient, including nontidal freshwater floodplain swamps bordering the estuarine boundary, past the head of tide into TFFWs and down to the lowest extent of forested wetlands. There, salinity and hydroperiod have transitioned the tidal forests into oligohaline marshes [15,19,24,25], and the remnant standing dead trees are referred to as "ghost forests". This gradient represents a space-for-time substitution design, allowing inference of potential migration of lower estuary wetland systems to more upstream locations with future sea level rise (SLR) [15,16,24,26]. The relative SLR on the lower Atlantic coastal plain has averaged 3.5 mm yr^{-1} since the 1920s (NOAA gauge 8665530, Charleston, South Carolina), but regional accelerations as high as 9.8 mm yr^{-1} have been reported in the Southeastern US [27]. Modeling efforts based on similar SLR rates predict an increase of 14% in the area occupied by nontidal swamps and a decrease of 24% in the area occupied by TFFWs in the Southeastern US over the next 100 years [26]. Historical data for all blue C ecosystems indicate annual decreases in spatial extent of 0.7%–7%, due primarily to land-use changes [1]. Thus, regional rates of loss reported by Craft et al. [26] strongly exceed rates from other blue C ecosystems due primarily to damming, diking, ditching, and development.

Assessments of spatial C allocation across UEFWs are exceedingly rare [2,4,11], except for recent work in blue C systems such as tidal marshes and seagrass beds [1,5]. While the majority of C is stored belowground in blue C ecosystems [28], aboveground biomass dynamics are more uncertain in time owing to episodic events and stress-imposed structural shifts. However, as noted by the Global Climate Observing System, aboveground biomass is a critically important variable in linking C dynamics to climate modeling [18]. The temporal dynamics of aboveground C have been investigated in many other blue C ecosystems (e.g., [29,30]) but not for UEFWs. Here, we contribute to filling this research gap by investigating three new aspects of aboveground C dynamics for UEFWs. First, we extend a pre-existing record of aboveground C change on the Winyah and Savannah systems [4]. This previous study raised concern for how rapidly aboveground C changes may occur along these and other transitional UEFW environments both naturally and in model simulations (e.g., [31]) by reporting changes in total aboveground C of between +15.1% to −74.4% over a 7-year period and changes in standing dead biomass of as much as 142%. We extend this record for another 8–10 years to focus specifically on this metric of change. Second, we augment the landscape context for aboveground C storage by adding sites farther inland where we hypothesize that future sea-level-rise-driven change is imminent. Third, we add to the salinity-stress literature, which often focuses on seedlings [32], by adding information on how salinity affects the coastal C balance at the ecosystem scale.

2. Materials and Methods

UEFW C standing stocks were assessed on two series of 5 study sites each along estuarine gradients of both the Savannah River and the Winyah Bay systems, which comprise sites on the Waccamaw, Pee Dee, and Sampit Rivers. This study leveraged three pre-existing UEFW research areas per system, which were established in 2004 and exhibit hydrologic conditions including semidiurnal tidal inundation and ranging from oligohaline to entirely freshwater [20]. In 2020, two additional study areas were established on each estuary system to include an area near the upper extent of tidal influence that has a seasonal belowground tidal signature ("head of tide") and an area that experiences no tidal flooding throughout the year ("nontidal"), but which still experiences tidal influence within the channel of the adjacent river (Figure 1). These new sites add to the landscape context of the original 3-site series. Each study site contained two 20 × 25 m subplots which

included 2 water monitoring wells and five 0.25 m^2 litter traps. Long-term soil porewater salinity conditions at the 3 estuarine sites were previously described [4], ranging from exceeding 4.0 ppt at heavily salt-impacted UEFWs ("lower" sites), to generally 1.2–1.4 ppt at moderately salt-impacted UEFWs ("middle" sites), and very low or nonexistent salinity (~0.1 ppt) at continuously fresh UEFWs ("upper" sites). The data for this study were collected from the summer of 2020 to the spring of 2022.

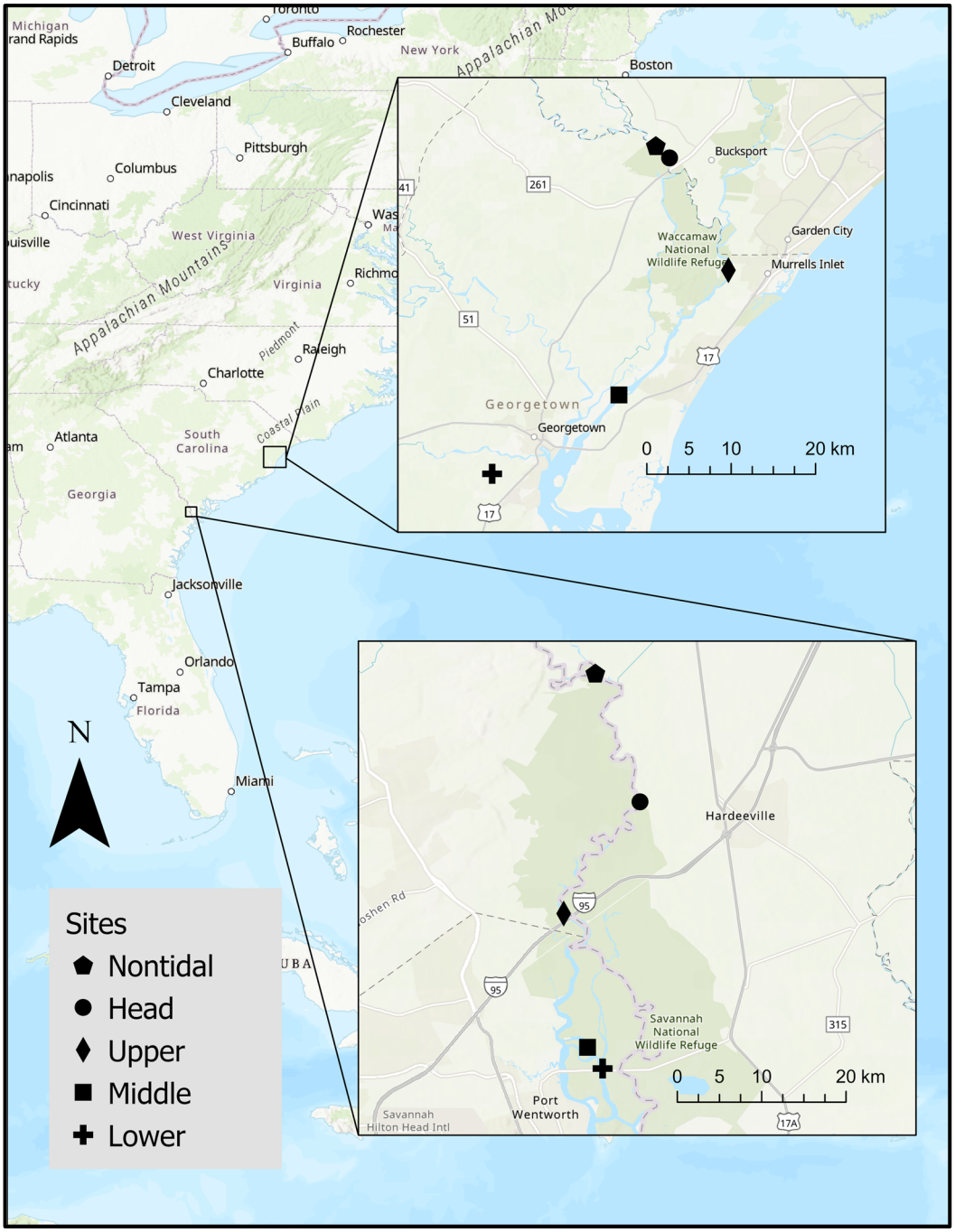

Figure 1. Site locations within the southeastern Atlantic coast of the United States, including the Savannah River, Georgia, and Winyah Bay, South Carolina.

Porewater salinity was measured monthly using a handheld water quality instrument (model Pro30, YSI Inc., Yellow Springs, OH, USA). Four salinity monitoring wells were installed near the corners of the plots. The monitoring wells were constructed from 3.2 cm

diameter slotted Schedule 40 PVC with the bottom end of the well permanently capped but vented. These wells were inserted to a depth of ~60 cm, and all the wells were slotted and wrapped in a fiberglass screen to help reduce the infiltration of sediments. Any residual water was pumped out of the wells, which were allowed to refill before salinity was measured. The heights of the wells above the ground varied to allow researchers access during flooding events. The water level data were collected using a continuously deployed non-vented pressure transducer (models LT/LTC 3001 and Levelogger Edge M10, Solinst Canada Ltd., Georgetown, ON, Canada) which were post-processed using atmospheric pressure data collected simultaneously from on-site barometric pressure sensors (model LT 3001 Barologger Edge M1.5, Solinst Canada Ltd., Georgetown, ON, Canada).

Carbon stocks of trees, snags, shrubs, and saplings were estimated using the Forest Inventory Analysis Component Ratio Method (FIA-CRM) as established by the US Forest Service [33]. Many authors in the allometric modeling field have argued that uncertainty related to the selection of allometric equations (i.e., species-specific vs. generic models) contributes significantly to modeling errors [34–37]. It is likely that trees in transitional environments such as salinity-impacted swamps exist in conditions that deviate from established allometry, thus contributing a potential source of error [17,34]. Nonetheless, the need for standardization is clear in the context of nationwide datasets with which we intend our UEFW observations to be compatible [17,38]. For this reason, we chose to use the FIA-CRM rather than generic (i.e., [39]) or simple linear (i.e., [38]) methods of allometry.

To assess total aboveground C stocks, we measured live trees, live shrubs, live saplings, live and dead herbs, litterfall, standing dead trees, coarse woody debris (CWD), and fine woody debris (FWD). Woody stem measurement in our study follows the methods laid out in the FIA field guide 9.0 [33]. Stems within our plots were sorted by size into trees, saplings, shrubs, and snags during the analysis. All live woody stems greater than 2.5 cm diameter at breast height (DBH, 1.3 m aboveground) and taller than 1.3 m were DBH-measured. The height of each stem was measured using a digital hypsometer (models Vertex IV and Transponder T3, Haglof Inc., Långsele, Sweden). The diameters were measured using standard D-tapes when the stems were larger than 2.5 cm, while analog calipers were used for smaller stems. The levels of decay on dead standing trees were estimated following Domke et al. [40]. The percentage cull for snags was estimated based on decay class: classes 1 and 2 were 0%, class 3 was 20%, class 4 was 50%, and class 5 was 75%. Dead trees (snags) were not included in the survey if their DBH was <10.0 cm. Due to the frequently flooded nature of our plots, we placed less subjective weight on a snag's basal decay than is indicated in Domke et al. Table 1 [40], under the assumption that rot at the base of a snag was accelerated by site conditions and did not accurately reflect the decay state of the entire bole.

The biomass (kg) of the woody stems was calculated using the component ratio method (CRM) as established by Woodall et al. [41] and adopted by the US Forest Inventory Analysis [33] program. In this method, tree height, diameter, and cull are figured into region- and species-specific equations to calculate the biomass of stems including bark and stumps, but not foliage. The classification of small woody stems as either shrubs or saplings is a noted source of discrepancy between researchers [42]. In this study, all woody specimens were sorted by stem diameter alone; trees were defined as any stem $\geq$10.0 cm DBH, saplings were defined as any stem between 2.5 cm and 10 cm DBH, and shrubs were defined as any stem that was <2.5 cm DBH but $\geq$2.5 cm at 0.3 m above the root collar. While this results in some very small saplings being treated as shrubs and some large specimens of stereotypical shrubs being treated as saplings, it is necessitated by the fact that the equations used for our smallest specimens (shrubs) are calibrated for relatively small DBH (<2.5 cm) values, while sapling and tree equations do not function when DBH inputs are under their intended cutoff values (12.5 and 2.5 cm DBH, respectively) [42]. Sapling biomass was calculated according to Heath et al. [42], which adapts the CRM to smaller stem sizes seen in this size class. Shrub biomass was calculated using a generalized hardwood model [43], which permits the calculation of even smaller stems than the Heath

method. Snag biomass was calculated according to Domke et al. [40]. All the live wood biomass was assumed to be 50% C by dry weight.

Foliar biomass (Mg C ha^{-1}) was measured for each site using ten 0.25 m^2 litter traps distributed evenly throughout the area. The litter traps were approximately 1.2 m tall and thus represent both overstory and understory woody plant litterfall. Samples were collected monthly between April 2021 and March 2022 and dried at 70 °C for at least 3 days before weighing. Foliar mass was also assumed to be 50% C by dry weight, as established by previous work in the system [4]. Average monthly litter weights (g C m^{-2}) were then summed across the study duration to assess the total annual foliar production at a given site, which is treated as the plot's foliar standing stock in Mg C ha^{-1}.

The understory herbaceous stocks were estimated following the methodology of Ensign et al. [24]. Herbaceous plants were sampled quarterly between spring 2021 and winter 2022 utilizing two 25 m transects perpendicular to the river channel placed outside our existing forest inventory plots, making them ~50–100 m apart. Five 0.25 m^2 plots were located pseudo-randomly along each transect. The species within the plot were identified, sorted into live and dead biomass, dried at 70 °C for ≥5 days, and weighed. The herbaceous biomass for each site was calculated by averaging the ten samples per site for each season. The four seasonal herbaceous values were then averaged to annualize the herbaceous C standing stock. The herbaceous dry mass values were converted to C using established ratios [4] of 38.35% C for live mass, and 36.25% C for necromass. Necromass and live mass were both included in the herbaceous biomass inventory values.

Downed woody debris (DWD) was measured using the line-intercept technique originally presented by Van Wagner [44]. In each site, 20 m transects originating from the centers of the two subplots were established. We divided each subplot into quarters, delineated by the cardinal directions as measured from the center point; a transect was placed within each quarter along a random heading. In this way, 4 transects per subplot were established in an attempt to overcome the high variability often observed in DWD data [12]. Along the full length of each transect, all debris with a diameter > 7.5 cm ("coarse woody debris", CWD) was recorded for diameter and decay class. Decay class was separated into one of three categories: sound, intermediate, and rotten. Sound debris was fresh and possessed no detectable decay, while rotten wood was easily penetrated by measurement calipers [45]. For the first 4 m of the transect, fine woody debris with diameters between 1 cm and 7.5 cm were tallied. Ultra-fine woody debris with a diameter <1 cm was tallied for the first 2 m of the transect as well. These two classes are referred to collectively as fine woody debris (FWD). The total mass of DWD was calculated at line intercept, where each debris fragment's volume (V) in m^3 is calculated by the following formula:

$$V = \left[\pi^2 \left(\sum {d_i}^2\right) / 8\ L\right] \times k \quad (1)$$

where d_i is the diameter of a fragment in m, L is the sample line's length in m, and k is the per-ha conversion constant [44]. As our data for fine and ultra-fine debris were tallied based on size class, these counts were assumed to have the median value for their range. Fine woody debris was assumed to be 4.25 cm in diameter, and ultra-fine was assumed to be 0.5 cm in diameter.

To extend and examine the pre-existing record of aboveground C change and the influence of salinity on the three sites for which data has been previously reported ("upper", "middle", and "lower") [4], a simple linear regression was run between the % change in tree carbon between each 7-year time step and the average salinity therein. Only tree C was assessed for this analysis due to irregular time steps in the collection of other C pools such as vegetation and DWD. The data available at these sites are neither normally distributed (according to Shapiro–Wilk testing, salinity is non-normal) nor extensive enough (n = 12) to allow for more robust statistical hypothesis testing or modeling methods; however, the slope of this simple regression is unbiased and provides a reasonable first

estimation of aboveground tree C stock loss per unit change in salinity in the UEFWs of the Southeastern US.

3. Results

On the Savannah River, salinity ranged from 1.6 to 6.5 ppt (avg 3.4 ppt) on the most seaward site ("lower"), and 0.2 to 1.3 ppt (avg 0.4 ppt) on the next site upriver ("middle"). Similarly, salinity values on the Winyah system were 0.4–4.1 ppt (avg 1.6 ppt) on the "lower" site and 0.1–2.2 ppt (avg 0.5 ppt) on the "middle". Salinity values on the "upper", "head of tide", and "nontidal" sites on both systems were consistently low, averaging below 0.2 ppt throughout the study duration. Inundation patterns varied across the estuarine gradient, driven by river flow rates and the low relief of the southeastern coastal plain. Sites toward the riverine boundary of the estuary ("nontidal" and "head of tide") tended to be dominated by low-frequency, high-duration flooding, while sites on the seaward side of the estuarine gradient ("upper", "middle", and "lower") were defined primarily by semidiurnal tidal cycles (Figure 2). The water levels at tidal sites ("upper", "middle", and "lower") on the Savannah River showed a range of −0.5–0.5 m relative to the soil surface, while on the Winyah River, they fluctuated by −1.5–1.1 m across the duration of the study. The water levels at "nontidal" and "head of tide" sites on the Savannah River ranged from −1.4 to 1.3 m, while on the Winyah River, they ranged from −0.4 to 1.2 m. The "upper" sites on both rivers were just upstream of salinity intrusion, showing negligible porewater salinity values akin to the "nontidal" and "head of tide" sites, but still within the elevational range to be subject to semidiurnal tides akin to the "middle" and "lower" sites.

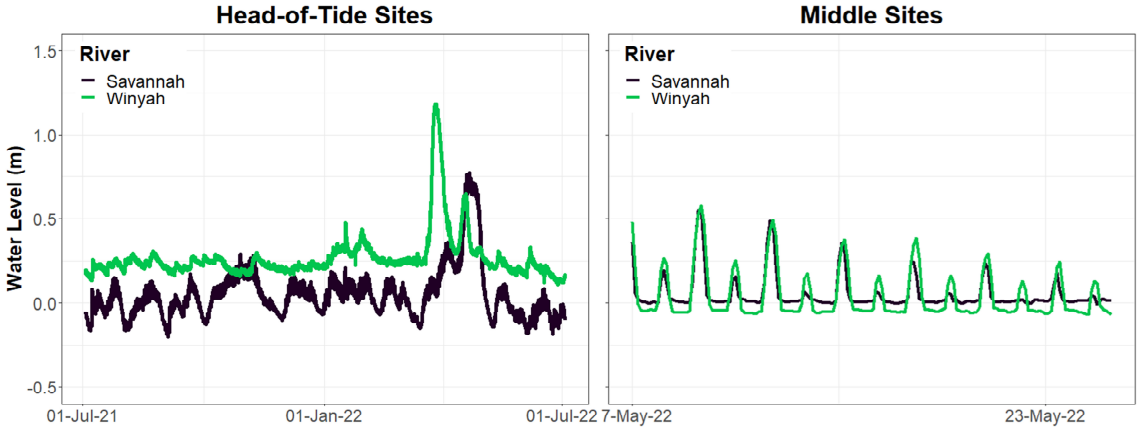

Figure 2. Water level patterns vary across the estuarine gradient of the systems, being characterized as either low-frequency, high-magnitude (**left**), or semidiurnal (**right**) flood patterns. Note that the two hydrographs show different temporal scales on the x-axes, but the same meter scale on the y-axes, and retain the same color designation for each river throughout.

On the Savannah River, the total aboveground C storage in vegetation ranged from 28.1 Mg C ha^{-1} to 287.0 Mg C ha^{-1}. On the Winyah system, the total C values ranged from 38.0 Mg C ha^{-1} to 221.6 Mg C ha^{-1}. Both rivers showed markedly similar total C values across their UEFW gradient (Table 1). On both systems, we observed the expected decrease in aboveground C corresponding with the increasing salinity of the lower-estuary plots ("lower" and "middle" sites, Figure 3). On all the sites except for one (Savannah "lower"), trees dominated the total aboveground C makeup of our plots, accounting for an average of 88.2% of aboveground C. Savannah "lower" has had near complete die-off of trees since its original establishment in 2005, and consequently trees accounted for only 9.5% of aboveground biomass there, with the majority of C being stored instead in standing snags (16.9 Mg C ha^{-1}, 60.1%).

Table 1. Carbon (C) stocks at study sites along the Winyah and Savannah systems.

	Winyah					Savannah				
	Nontidal	**Head**	**Upper**	**Middle**	**Lower**	**Nontidal**	**Head**	**Upper**	**Middle**	**Lower**
Total aboveground C	217.2	221.6	210.8	123.7	38.0	287.0	207.8	222.7	172.2	28.1
Live Trees	197.0	192.0	200.0	111.9	23.9	254.1	189.1	208.0	164.0	2.7
Saplings	1.7	5.4	1.8	0.3	0.2	2.0	1.3	4.1	0.2	0.0
Shrubs	0.00	0.00	0.15	0.02	0.00	0.27	0.00	0.66	0.00	0.57
Foliage	3.16	2.48	3.49	2.39	0.43	2.92	2.51	2.51	1.55	--
Herbs	0.01	0.00	0.26	0.87	1.04	0.05	0.05	0.24	0.49	4.04
Snags	1.3	7.8	0.4	1.7	9.9	0.0	6.8	2.0	1.5	16.9
FWD	11.9	11.1	3.6	5.0	1.3	13.8	4.2	4.3	3.6	1.7
CWD	2.1	2.8	1.1	1.5	1.3	13.8	3.8	1.0	0.8	2.2
Mean Salinity (psu)	0.2	0.2	0.1	0.5	1.5	0.1	0.2	0.1	0.5	3.7
Range	(0.1–0.2)	(0.1–0.3)	(0.0–0.1)	(0.2–1.9)	(0.3–3.6)	(0.0–0.1)	(0.1–0.2)	(0.1–0.3)	(0.2–1.0)	(1.8–5.4)

Values represent average Megagrams of carbon per hectare (Mg C ha^{-1}) of a given biomass pool in each of our sites. Two subplots per location were averaged. The Savannah "lower" site did not have enough trees to warrant the placement of litter traps and therefore does not have a foliage value. FWD; fine woody debris. CWD; coarse woody debris.

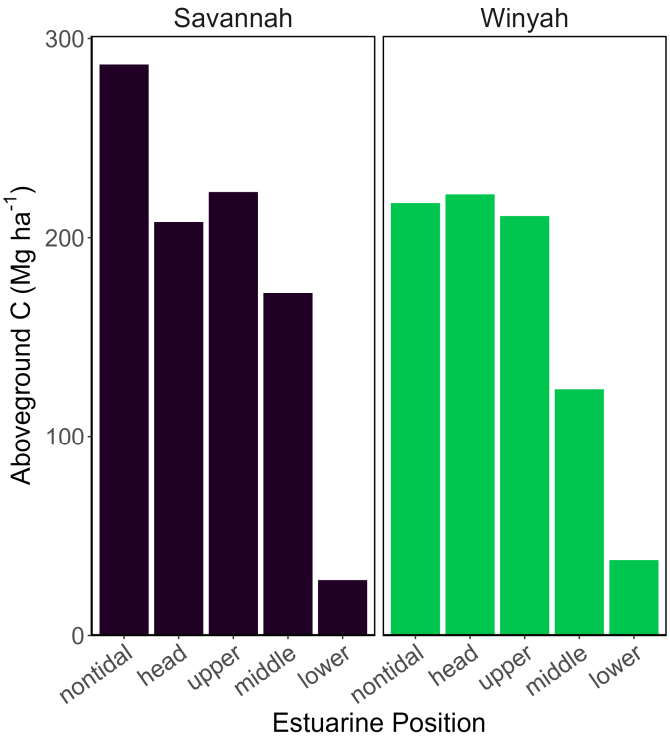

Figure 3. Observed total aboveground carbon (Mg C ha^{-1}) by estuary position of every individual plot.

On all the plots, bald cypress (*Taxodium distichum* L. Rich.) and water tupelo (*Nyssa aquatica* L.) dominated the live tree C biomass pools, except for "lower" plots where water tupelo has been excluded by excessive porewater salinity (Table 2). Associate species such as swamp tupelo (*Nyssa biflora* Walter), red maple (*Acer rubrum* L.), ash (*Fraxinus* spp.), and water elm (*Planera aquatica* J.F. Gmel.) were common, but rarely rose above 10% of overall tree C, with the notable exceptions taking place at the "upper" plots, where moderate stress may be driving higher diversity. Herbaceous C was distributed across a higher number of species, with no single species contributing more than 35% of overall yearly C (Table 3).

Table 2. Tree species contributions to standing biomass stocks.

	Nontidal			Head			Upper			Middle			Lower		
Winyah	**Species**	**C (Mg/ha)**	**%**	**Species**	**C (Mg/ha)**	**%**	**Species**	**C (Mg/ha)**	**%**	**Species**	**C (Mg/ha)**	**%**	**Species**	**C (Mg/ha)**	**%**
	w.tupelo	102.85	52.2	w.tupelo	115.59	60.21	baldcypress	161.61	80.79	baldcypress	109.13	97.52	baldcypress	23.94	100.00
	baldcypress	93.25	47.35	baldcypress	54.82	28.56	red maple	21.03	10.52	w. tupelo	1.53	1.37			
	water elm	0.74	0.37	water elm	6.88	3.58	s. tupelo	17.16	8.58	s. tupelo	1.24	1.11			
	red maple	0.12	0.06	laurel oak	4.64	2.42	ash	0.18	0.09						
				s. cottonwood	2.47	1.29	laurel oak	0.03	0.02						
				ash	2.43	1.26	waxmyrtle	0.02	0.01						
				white oak	1.70	0.88									
				sweetgum	1.54	0.80									
				red maple	1.24	0.64									
				s. tupelo	0.51	0.27									
				deciduous holly	0.15	0.08									
	Nontidal			**Head**			**Upper**			**Middle**			**Lower**		
Savannah	**Species**	**C (Mg/ha)**	**%**	**Species**	**C (Mg/ha)**	**%**	**Species**	**C (Mg/ha)**	**%**	**Species**	**C (Mg/ha)**	**%**	**Species**	**C (Mg/ha)**	**%**
	baldcypress	130.41	51.33	baldcypress	91.59	48.44	baldcypress	91.74	44.11	baldcypress	162.65	99.17	baldcypress	2.35	88.54
	w. tupelo	115.72	45.55	w. tupelo	83.13	43.97	w. tupelo	63.26	30.42	s. tupelo	1.36	0.83	c. tallow	0.30	11.46
	red maple	5.95	2.34	s. tupelo	7.97	4.22	s. tupelo	34.98	16.82						
	a. elm	1.27	0.50	red maple	4.23	2.24	laurel oak	8.67	4.17						
	water elm	0.57	0.22	ash	1.56	0.82	red maple	5.63	2.71						
	hornbeam	0.11	0.04	sweetgum	0.35	0.19	water oak	2.04	0.98						
	hawthorn	0.05	0.02	water elm	0.23	0.12	ash	1.57	0.76						
							american elm	0.10	0.05						

All species present are included. Latin binomials are available in Table S1.

Table 3. Herbaceous species contribution to standing biomass stocks.

	Nontidal			Head			Upper			Middle			Lower		
Winyah	**Species**	**C (Mg/ha)**	**%**	**Species**	**C (Mg/ha)**	**%**	**Species**	**C (Mg/ha)**	**%**	**Species**	**C (Mg/ha)**	**%**	**Species**	**C (Mg/ha)**	**%**
	panicgrass	0.22	30.62	whitegrass	0.06	68.18	sensitive fern	2.56	19.49	waterparsnip	9.01	22.30	cattail	6.90	23.28
	whitegrass	0.10	13.52	unknown	0.03	31.82	lizards tail	1.85	14.03	giant cutgrass	7.60	18.81	giant cutgrass	3.13	10.56
	beaksedge	0.09	12.10	necromass	0.00	0.00	annual wildrice	1.08	8.20	seaside goldenrod	5.21	12.89	annual wildrice	3.12	10.54
	clearweed	0.05	7.56				halberdleaf	0.74	5.61	annual wildrice	1.99	4.92	softstem bulrush	2.64	8.91
	Elliot's ast.	0.05	7.20				water hemlock	0.73	5.52	water hemlock	1.63	4.03	cordgrass	1.82	6.15
	necromass	0.00	0.00				necromass	0.36	2.73	necromass	1.17	2.90	necromass	5.66	19.11
	Nontidal			**Head**			**Upper**			**Middle**			**Lower**		
Savannah	**Species**	**C (Mg/ha)**	**%**	**Species**	**C (Mg/ha)**	**%**	**Species**	**C (Mg/ha)**	**%**	**Species**	**C (Mg/ha)**	**%**	**Species**	**C (Mg/ha)**	**%**
	carex	2.32	27.93	panicgrass	1.11	22.83	giant cutgrass	2.90	25.52	cattail	2.79	18.30	cordgrass	24.90	34.83
	panicgrass	2.25	27.11	marsh seedbox	0.83	17.07	haspan flatsedge	1.48	13.00	Virginia peltandra	2.33	15.28	giant cutgrass	10.95	15.33
	cordgrass	1.52	18.38	Lizards tail	0.80	16.52	cordgrass	1.24	10.87	giant cutgrass	1.65	10.86	cattail	10.80	15.11
	lizards tail	0.86	10.39	s. smartweed	0.67	13.86	panicgrass	1.24	10.91	sturdy bulrush	1.58	10.34	sturdy bulrush	1.76	2.46
	beaksedge	0.75	9.04	seedbox	0.29	5.96	carex	0.64	5.62	lizards tail	0.81	5.31	bur marigold	1.75	2.45
	necromass	0.24	2.92	necromass	0.85	17.56	necromass	0.60	5.64	necromass	0.82	5.38	necromass	19.40	27.14

Only the top 5 species by mass (except where <5 species were observed) and necromass values in each plot are listed. Latin binomials are available in Table S1.

In our plots, we observed that herbaceous C pools were negligible in sites approaching the uppermost estuarine extent ("nontidal" and "head of tide" sites), ranging from 0.0% to 0.26% of non-tree aboveground C in these areas (Figure 4). The herbaceous C pool became much more meaningful in the semidiurnally tidal plots towards the seaward side of our estuarine gradient, increasing from 1.7% in continuously freshwater tidal forest ("upper" sites) to 15.9% in oligohaline tidal forest converting to tidal marsh (lower sites). When CWD and FWD are added together to represent all downed woody debris (DWD), this pool takes up between 15.4% and 83.9% of non-tree biomass across the estuarine gradient. Sites at the uppermost estuarine extent tended to have more DWD, while seaward estuarine sites showed a higher proportion of their non-tree biomass in still-standing snags. Snags made up 70.2% and 66.4% of non-tree biomass in Winyah and Savannah "lower" sites, respectively. Snags also had large contributions to biomass in the "head of tide" sites, accounting for 26.2% of non-tree biomass on the Winyah River and 36.3% on the Savannah River. Foliage made up between 3.0% and 32.4% of non-tree biomass in all the plots other than Savannah "lower", with this mass corresponding tightly to tree biomass. Sapling biomass was nearly non-existent in the "lower" and "middle" sites, ranging from 0.0% to 3.1%. Sapling biomass increased in the "upper", "head of tide", and "nontidal" sites, where biomass ranged from 6.2% to 27.8% of non-tree C.

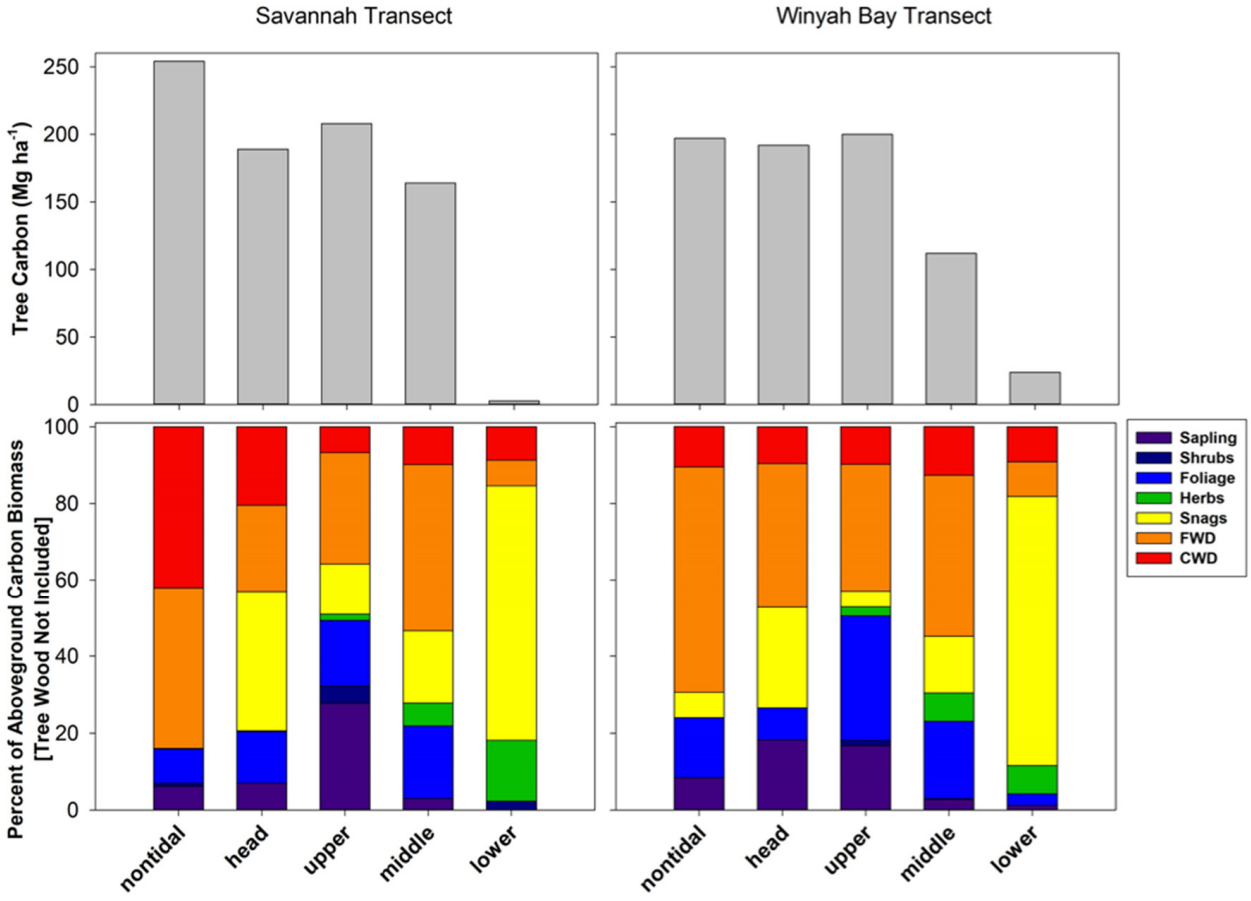

Figure 4. (**Top**) Tree carbon (C) in Megagrams per hectare by river position. (**Bottom**) Percent contribution of each biomass pool to the given plot's total C, barring live mature trees.

4. Discussion

With total aboveground C stocks on the Savannah River and within the Winyah estuary averaging 172.9 Mg C ha^{-1} and ranging from 28.1 to 286.9 Mg C ha^{-1}, storage rates in these southeastern deepwater swamps appear broadly comparable to those values found by other efforts in similar systems (Table 4). The community composition of our sites closely matches the *Taxodium*/*Nyssa* association described for the southeastern coastal plains [15], and aboveground biomass thereon is stored overwhelmingly in live trees, followed by either DWD or snags (Table 1). As UEFWs are not yet routinely delineated in terms of national- or global-scale C accounting, these ecosystems are nested within the southeastern oak/gum/cypress forest designation used by the United States Department of Agriculture's (USDA) Forest Inventory and Analysis (FIA) database [46], or within the IPCC's designation as "American humid subtropical forest", where "American" refers to both the northern and southern American continents [47,48]. The Southeastern US UEFWs measured here show significantly higher storage capacity in comparison to either of these broader benchmarks and are roughly analogous to the UEFWs found in the northwestern US (Table 4). The comparatively high C storage rates found in the "head of tide" and "nontidal" sites in this study provide support for their consideration as UEFWs, in addition to those sites already established by previous work [4], in turn supporting the expansion of the spatial extent of UEFWs in the US Southeast to include locations only rarely impacted by tidal forces, analogous to supratidal wetlands [10]. These ecosystems on the uppermost extent of current tidal influence are likely to experience more frequent tidal events under the predicted impacts of climate change [16,27], driving the need to understand these future loci of critical ecosystem migration.

Table 4. Ranges (or averages ± SD where ranges were not presented) of aboveground carbon (C) reported in the present study and relevant benchmark ecosystems.

Region	Aboveground C (Mg ha^{-1})	Source
Southeastern US UEFWs (deepwater swamps)	55.9–184.7 [a]	Krauss et al. [4]
	68.5–177.0 [b]	Ricker et al. [12]
	28.1–286.9	Present work
Northwestern US UEFWs (spruce swamps)	74–395 [c]	Kauffman et al. [2]
Southeastern oak/gum/cypress forests	72.9 ± 52.4 [d]	USDA database [46]
IPCC American subtropical humid forest	39.7 ± 20.2 [e]	Rozendaal et al. [47]

All values in aboveground dry C, including live mass and necromass. Inclusion or exclusion of roots and stumps as well as allometric method selection varies slightly across studies, contributing some amount to observed variations. [a]: Values from Krauss et al. (Table 1) [4], excluding "Marsh" sites. [b]: Values from Ricker et al. (Table 5) [12] include stumps and utilized diameter-only allometry [39]. [c]: Range of aboveground C stock in "tidal forests" only. [d]: Obtained 6 June 2024 [46]. Includes surveys from South Carolina and Georgia from 2015 to 2022. See Hoover and Smith [49] for further exploration. [e]: Values from Rozendaal et al. (Table 1) [47], converted from aboveground biomass to C by multiplying by their reported conversion factor of 0.47. Includes both North and South Americas.

Our extension of the previous work on these systems provides evidence that salinity intrusion of relatively low magnitude (~1.0 ppt) can result in meaningful loss of aboveground biomass in southeastern UEFWs, potentially driving much of the observed rapid changes in aboveground C that prompted the initiation of this project [4]. C storage in trees at "middle" plots on both the Winyah and Savannah systems maintained equilibrium (+0.8%) or incurred minor losses (−5.5%), respectively, between 2005 and 2012 when their salinities averaged 1.5 ppt, but experienced C increases (+19.2%, +40.2%, resp.) between 2013 and 2020 when relatively fresh (avg = 0.65 ppt) conditions prevailed (Table 5). "Lower" sites, which were originally established at the lowest extent of the UEFW ecological range, were observed to completely transition from forests to oligohaline marshes, with consistent losses of live tree biomass ranging from −22 to 75% over 7-year time steps and community

composition in 2021 dominated by genera such as *Spartina*, *Typha*, and *Zizaniopsis* (Table 3). "Upper" sites on both rivers, which experienced no salinity intrusion, demonstrated highly variable (ranging from +6.8% to +45.7%) but consistently positive (avg = 19.7%) tree growth across all three observational studies of the systems. These observations, especially the apparent release of growth at bald cypress-dominated "middle" sites (Table 2) in response to a low magnitude but consistent decrease in interstitial salinity, demonstrate the plasticity of response by bald cypress trees to cope with low levels of salinity.

Table 5. Comparison of codominant tree carbon (C) values from Krauss et al. [4] and the current work.

River	Position	2005		2012		2020	
		sal	Mg C ha^{-1}	*'06–'12 sal*	Mg C ha^{-1} (Δ %)	*'13–'20 sal*	Mg C ha^{-1} (Δ %)
Winyah	Nontidal		n/a		n/a		197.0
	Head		n/a		n/a		192.0
	Upper	*0.1*	128.6	*0.1*	137.3 (+6.8%)	*0.1*	200 (+45.7%)
	Middle	*0.8*	93.2	*1.7*	93.9 (+0.8%)	*0.7*	111.9 (+19.2%)
	Lower	*1.9*	49.9	*2.7*	30.6 (−38.7%)	*1.5*	23.9 (−21.9%)
Savannah	Nontidal		n/a		n/a		254.1
	Head		n/a		n/a		189.1
	Upper	*0.1*	162.6	*0.1*	187.1 (+15.1%)	*0.1*	208.0 (+11.2%)
	Middle	*0.6*	123.8	*1.3*	117.0 (−5.5%)	*0.6*	164.0 (+40.2%)
	Lower	*2.5*	42.2	*4.3*	10.8 (−74.4%)	*3.8*	2.7 (−75.0%)

Interim salinity values in ppt from 2005–2012 are recalculated with slightly different temporal ranges from data previously published in Krauss et al. [4]. Note that 2020 C values used height- and diameter-based allometry [41], while previous work used diameter-only equations [39], which accounts for some of the observed variations.

A preliminary assessment of the magnitude of salinity's effect suggests that a chronic 1 ppt increase in groundwater conditions may reduce aboveground tree C by approximately 26% (Figure 5). While the data and conclusions drawn from these sites are limited in scope, this simple linear regression analysis provides a preliminary estimation of the magnitude and directionality of salinity-induced aboveground tree C stock change in the UEFWs of the Southeastern US. The expected drivers of this loss include the direct imposition of osmotic stress by the presence of salinity [4,21], as well as the concurrent sulfide-induced transition from a methanogenic soil condition to a sulfate-reducing condition [19] and the structural changes incurred by resultant shifts in vegetation. Soil condition and porewater salinity have been shown to have significant impacts on not only overall stand density and community [25] but also resource partitioning by plants under stress [50,51]. Similarly, salinity changes of 1 ppt have also been shown to reduce tree water use by roughly 20% [32], indicating a potential coupling of consistent magnitude between water use and C storage capacity. The trees in our sites exist along salinity gradients that can cause a reduction in canopy crown size, which is associated with lower individual tree water use and growth rates, and is analogous to crown sizes in highly competitive stands [32]. Freshwater swamps, as well as other floodplains, have been found to contain more dead woody debris than upland forests [12,52], which may drive additional C storage in these systems. Our data also suggest that the abundance of woody debris, both fine and coarse, is inversely related to salinity (Table 1), despite the opposite being true for the abundance of standing dead snags (Figure 4). This is potentially explained in part by greater tidal flushing and less obstruction by stems and hummocks at downstream sites leading to greater export rates, although the noted high variance in dead wood survey methods [12,53] suggests that these trends require a more focused study design to assess with greater confidence.

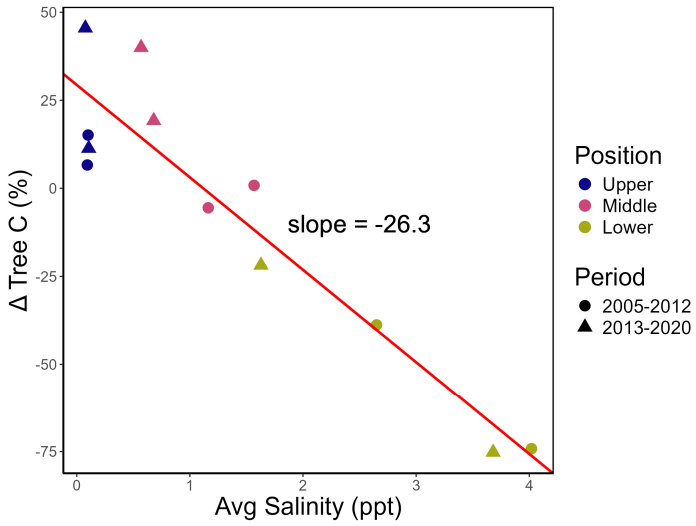

Figure 5. The % change in aboveground tree carbon (C) between sampling years and the average salinity across the intervening years (Table 5). This simple linear regression fails to fully account for the repeated measures data structure and should be interpreted with caution, but provides a preliminary value of an approximately 26% loss in tree C per 1 ppt.

5. Conclusions

We investigated three aspects of aboveground C dynamics in the UEFWs of the Southeastern US. In the pursuit of our first goal to extend the observational record of these UEFW sites, we replicated earlier studies on the same systems, again finding rapid changes in ecosystem C. In this timeframe (2012–2021), changes in tree C ranged from +46% in freshwater sites to −75% in sites undergoing full transition into oligohaline marsh. Our data further suggest that salinity intrusion of magnitudes as low as 1 ppt can cause significant changes in aboveground C storage capacity and growth over sub-decadal timescales. Our efforts towards the second goal, the addition of sites farther inland at or just beyond tidal influence, provide novel assessments of highly C-dense ecosystems that are routinely poorly quantified. As sea levels rise, we can predict that these currently nontidal sites will trend towards the conditions observed at the more tidally influenced freshwater sites. More frequent freshwater inundation at nontidal sites and increasing salinity stress at freshwater sites may result in significant mobilization of C currently sequestered within woody biomass and reduction in aboveground C storage, although the latter is likely to be offset by the belowground productivity from encroaching marshes. Finally, our assessment of salinity stress at an ecosystem scale has suggested a decrease in aboveground C of about 26% per 1 ppt. While needing additional inference from other rivers, this metric presents great potential utility for land managers in the region interested in projecting changes in forest C storage with salinity intrusion onto their lands.

Supplementary Materials: The following supporting information can be downloaded at: https://www.mdpi.com/article/10.3390/f15091502/s1, Table S1: Common and latin names of all species identified.

Author Contributions: Conceptualization, J.A.D., K.W.K. and W.H.C.; methodology, investigation, and formal analysis, C.J.S. and J.A.D.; writing—original draft preparation, C.J.S.; writing—review and editing, J.A.D., K.W.K., W.H.C., G.B.N. and S.L.W.; analysis—statistical consulting, S.L.W.; funding acquisition, J.A.D. and W.H.C. All authors have read and agreed to the published version of the manuscript.

Funding: This study was supported by the U.S. Geological Survey Climate Research and Development Program. This work is also partially supported by NIFA/USDA under project number SC-17005313.

Data Availability Statement: The data presented in this study are available on request from the corresponding author.

Acknowledgments: We are grateful for the research partnerships provided by refuge managers, biologists, and support staff of the U.S. Fish and Wildlife Service, specifically M. Craig Sasser at Waccamaw NWR and William Russell Webb, Jane Griess, Lindsay Coldiron, and Chuck Hayes at Savannah NWR. We also thank Jason Luquire for permission to access his land, and Brian Williams for his creation of the Figure 1 map presented herein. Technical Contribution No. 7325 of the Clemson University Experiment Station. Any use of trade, firm, or product names is for descriptive purposes only and does not imply endorsement by the U.S. Government.

Conflicts of Interest: The authors declare no conflicts of interest.

References

1. McLeod, E.; Chmura, G.L.; Bouillon, S.; Salm, R.; Björk, M.; Duarte, C.M.; Lovelock, C.E.; Schlesinger, W.H.; Silliman, B.R. A Blueprint for Blue Carbon: Toward an Improved Understanding of the Role of Vegetated Coastal Habitats in Sequestering CO_2. *Front. Ecol. Environ.* **2011**, *9*, 552–560. [CrossRef] [PubMed]
2. Kauffman, J.B.; Giovanonni, L.; Kelly, J.; Dunstan, N.; Borde, A.; Diefenderfer, H.; Cornu, C.; Janousek, C.; Apple, J.; Brophy, L. Total Ecosystem Carbon Stocks at the Marine-Terrestrial Interface: Blue Carbon of the Pacific Northwest Coast, United States. *Glob. Chang. Biol.* **2020**, *26*, 5679–5692. [CrossRef]
3. Smith, P.; Adams, J.; Beerling, D.J.; Beringer, T.; Calvin, K.V.; Fuss, S.; Griscom, B.; Hagemann, N.; Kammann, C.; Kraxner, F.; et al. Land-Management Options for Greenhouse Gas Removal and Their Impacts on Ecosystem Services and the Sustainable Development Goals. *Annu. Rev. Environ. Resour.* **2019**, *7*, 40. [CrossRef]
4. Krauss, K.W.; Noe, G.B.; Duberstein, J.A.; Conner, W.H.; Stagg, C.L.; Cormier, N.; Jones, M.C.; Bernhardt, C.E.; Graeme Lockaby, B.; From, A.S.; et al. The Role of the Upper Tidal Estuary in Wetland Blue Carbon Storage and Flux. *Glob. Biogeochem. Cycles* **2018**, *32*, 817–839. [CrossRef]
5. Pendleton, L.; Donato, D.C.; Murray, B.C.; Crooks, S.; Jenkins, W.A.; Sifleet, S.; Craft, C.; Fourqurean, J.W.; Kauffman, J.B.; Marbà, N.; et al. Estimating Global "Blue Carbon" Emissions from Conversion and Degradation of Vegetated Coastal Ecosystems. *PLoS ONE* **2012**, *7*, e43542. [CrossRef]
6. Bridgham, S.D.; Megonigal, J.P.; Keller, J.K.; Bliss, N.B.; Trettin, C. The Carbon Balance of North American Wetlands. *Wetlands* **2006**, *26*, 889–916. [CrossRef]
7. Chmura, G.L.; Anisfeld, S.C.; Cahoon, D.R.; Lynch, J.C. Global Carbon Sequestration in Tidal, Saline Wetland Soils. *Glob. Biogeochem. Cycles* **2003**, *17*, 1–12. [CrossRef]
8. Thorhaug, A.; Gallagher, J.B.; Kiswara, W.; Prathep, A.; Huang, X.; Yap, T.K.; Dorward, S.; Berlyn, G. Coastal and Estuarine Blue Carbon Stocks in the Greater Southeast Asia Region: Seagrasses and Mangroves per Nation and Sum of Total. *Mar. Pollut. Bull.* **2020**, *160*, 111168. [CrossRef]
9. Lovelock, C.E.; Duarte, C.M. Dimensions of Blue Carbon and Emerging Perspectives. *Biol. Lett.* **2019**, *15*, 20180781. [CrossRef]
10. Adame, M.F.; Kelleway, J.; Krauss, K.W.; Lovelock, C.E.; Adams, J.B.; Trevathan-Tackett, S.M.; Noe, G.; Jeffrey, L.; Ronan, M.; Zann, M.; et al. All Tidal Wetlands Are Blue Carbon Ecosystems. *Bioscience* **2024**, *74*, 253–268. [CrossRef] [PubMed]
11. Noe, G.B.; Hupp, C.R.; Bernhardt, C.E.; Krauss, K.W. Contemporary Deposition and Long-Term Accumulation of Sediment and Nutrients by Tidal Freshwater Forested Wetlands Impacted by Sea Level Rise. *Estuaries Coasts* **2016**, *39*, 1006–1019. [CrossRef]
12. Ricker, M.C.; Blosser, G.D.; Conner, W.H.; Lockaby, B.G. Wood Biomass and Carbon Pools within a Floodplain Forest of the Congaree River, South Carolina, USA. *Wetlands* **2019**, *39*, 1003–1013. [CrossRef]
13. Kelleway, J.J.; Adame, M.F.; Gorham, C.; Bratchell, J.; Serrano, O.; Lavery, P.S.; Owers, C.J.; Rogers, K.; Nagel-Tynan, Z.; Saintilan, N. Carbon Storage in the Coastal Swamp Oak Forest Wetlands of Australia. In *Wetland Carbon and Environmental Management*; Wiley: Hoboken, NJ, USA, 2021; pp. 339–353. ISBN 9781119639305.
14. Field, D.W.; Reyer, A.J.; Genovese, P.V.; Shearer, B.D. *Coastal Wetlands of the United States: An Accounting of a Valuable National Resource*; Oxford University: Oxford, UK, 1991; Volume 60.
15. Conner, W.H.; Doyle, T.W.; Krauss, K.W. *Ecology of Tidal Freshwater Forested Wetlands of the Southeastern United States*, 1st ed.; Springer Netherlands: Dordrecht, The Netherlands, 2007; ISBN 978-1-4020-5094-7.
16. Jia, G.; Shevliakova, E.; De Noblet-Ducoudré, N.; Houghton, R.; House, J.; Kitajima, K.; Lennard, C.; Popp, A.; Sirin, A.; Sukumar, R.; et al. *Land–Climate Interactions*; Bernier, P., Espinoza, J.C., Semenov, S., Eds.; Cambridge University Press: Cambridge, MA, USA, 2019; ISBN 9781009157988.
17. Houghton, R.A.; Hall, F.; Goetz, S.J. Importance of Biomass in the Global Carbon Cycle. *J. Geophys. Res. Biogeosci.* **2009**, *114*, G00E03. [CrossRef]
18. Santoro, M.; Cartus, O.; Carvalhais, N.; Rozendaal, D.M.A.; Avitabile, V.; Araza, A.; De Bruin, S.; Herold, M.; Quegan, S.; Rodríguez-Veiga, P.; et al. The Global Forest Above-Ground Biomass Pool for 2010 Estimated from High-Resolution Satellite Observations. *Earth Syst. Sci. Data* **2021**, *13*, 3927–3950. [CrossRef]
19. Hackney, C.T.; Avery, G.B. Tidal Wetland Community Response to Varying Levels of Flooding by Saline Water. *Wetlands* **2015**, *35*, 227–236. [CrossRef]

20. Krauss, K.W.; Duberstein, J.A.; Doyle, T.W.; Conner, W.H.; Day, R.H.; Inabinette, L.W.; Whitbeck, J.L.; Krauss, A.; Ken, W.; Jamie, A.; et al. Site Condition, Structure, and Growth of Baldcypress along Tidal/Non-Tidal Salinity Gradients. *Wetlands* **2009**, *29*, 505–519. [CrossRef]
21. Conner, W.H.; Krauss, K.W.; Doyle, T.W. Ecology of Tidal Freshwater Forests in Coastal Deltaic Louisiana and Northeastern South Carolina. In *Ecology of Tidal Freshwater Forested Wetlands of the Southeastern United States*; Springer: Dordrecht, The Netherlands, 2007; pp. 223–253; ISBN 9781402050947.
22. Doyle, T.W.; O'Neil, C.P.; Melder, M.P.V.; From, A.S.; Palta, M.M. Tidal Freshwater Swamps of the Southeastern United States: Effects of Land Use, Hurricanes, Sea-Level Rise, and Climate Change. In *Ecology of Tidal Freshwater Forested Wetlands of the Southeastern United States*; Conner, W.H., Doyle, T.W., Ken, K.W., Eds.; Springer Netherlands: Dordrecht, The Netherlands, 2007; pp. 1–28.
23. Duberstein, J.A.; Conner, W.H.; Krauss, K.W. Woody Vegetation Communities of Tidal Freshwater Swamps in South Carolina, Georgia and Florida (US) with Comparisons to Similar Systems in the US and South America. *J. Veg. Sci.* **2014**, *25*, 848–862. [CrossRef]
24. Ensign, S.H.; Hupp, C.R.; Noe, G.B.; Krauss, K.W.; Stagg, C.L. Sediment Accretion in Tidal Freshwater Forests and Oligohaline Marshes of the Waccamaw and Savannah Rivers, USA. *Estuaries Coasts* **2014**, *37*, 1107–1119. [CrossRef]
25. Davis, D.; DeRouen, M.; Roberts, D.; Wicker, K. *Assessment of Extent and Impact of Saltwater Intrusion into the Wetlands of Tangipahoa Parish, Louisiana*; NOS (National Ocean Service): Silver Spring, MD, USA, 1981; p. 59.
26. Craft, C.; Clough, J.; Ehman, J.; Jove, S.; Park, R.; Pennings, S.; Guo, H.; Machmuller, M. Forecasting the Effects of Accelerated Sea-Level Rise on Tidal Marsh Ecosystem Services. *Front. Ecol. Environ.* **2009**, *7*, 73–78. [CrossRef]
27. Parkinson, R.W.; Wdowinski, S. Geomorphic Response of the Georgia Bight Coastal Zone to Accelerating Sea Level Rise, Southeastern USA. *Coasts* **2023**, *4*, 1–20. [CrossRef]
28. Donato, D.C.; Kauffman, J.B.; Murdiyarso, D.; Kurnianto, S.; Stidham, M.; Kanninen, M. Mangroves among the Most Carbon-Rich Forests in the Tropics. *Nat. Geosci.* **2011**, *4*, 293–297. [CrossRef]
29. Safwan Azman, M.; Sharma, S.; Liyana Hamzah, M.; Mohamad Zakaria, R.; Palaniveloo, K.; MacKenzie, R.A. Total Ecosystem Blue Carbon Stocks and Sequestration Potential along a Naturally Regenerated Mangrove Forest Chronosequence. *For. Ecol. Manag.* **2023**, *527*, 120611. [CrossRef]
30. Kwan, V.; Fong, J.; Ng, C.S.L.; Huang, D. Temporal and Spatial Dynamics of Tropical Macroalgal Contributions to Blue Carbon. *Sci. Total Environ.* **2022**, *828*, 154369. [CrossRef]
31. Wang, H.; Dai, Z.; Trettin, C.C.; Krauss, K.W.; Noe, G.B.; Burton, A.J.; Stagg, C.L.; Ward, E.J. Modeling Impacts of Drought-Induced Salinity Intrusion on Carbon Dynamics in Tidal Freshwater Forested Wetlands. *Ecol. Appl.* **2022**, *32*, e2700. [CrossRef] [PubMed]
32. Duberstein, J.A.; Krauss, K.W.; Baldwin, M.J.; Allen, S.T.; Conner, W.H.; Salter, J.S.; Miloshis, M. Small Gradients in Salinity Have Large Effects on Stand Water Use in Freshwater Wetland Forests. *For. Ecol. Manag.* **2020**, *473*, 118308. [CrossRef]
33. U.S. Department of Agriculture. *Forest Service. Forest Inventory and Analysis National Core Field Guide*; Version 9.0; U.S. Department of Agriculture: Washington, DC, USA, 2019; Volume 1.
34. Vorster, A.G.; Evangelista, P.H.; Stovall, A.E.L.; Ex, S. Variability and Uncertainty in Forest Biomass Estimates from the Tree to Landscape Scale: The Role of Allometric Equations. *Carbon. Balance Manag.* **2020**, *15*, 8. [CrossRef]
35. Chave, J.; Réjou-Méchain, M.; Búrquez, A.; Chidumayo, E.; Colgan, M.S.; Delitti, W.B.C.; Duque, A.; Eid, T.; Fearnside, P.M.; Goodman, R.C.; et al. Improved Allometric Models to Estimate the Aboveground Biomass of Tropical Trees. *Glob. Chang. Biol.* **2014**, *20*, 3177–3190. [CrossRef]
36. Fonseca, W.; Alice, F.E.; Rey-Benayas, J.M. Carbon Accumulation in Aboveground and Belowground Biomass and Soil of Different Age Native Forest Plantations in the Humid Tropical Lowlands of Costa Rica. *New For.* **2012**, *43*, 197–211. [CrossRef]
37. Chaturvedi, R.K.; Raghubanshi, A.S. Aboveground Biomass Estimation of Small Diameter Woody Species of Tropical Dry Forest. *New For.* **2013**, *44*, 509–519. [CrossRef]
38. Clough, B.J.; Russell, M.B.; Domke, G.M.; Woodall, C.W.; Radtke, P.J. Comparing Tree Foliage Biomass Models Fitted to a Multispecies, Felled-Tree Biomass Dataset for the United States. *Ecol. Modell.* **2016**, *333*, 79–91. [CrossRef]
39. Jenkins, J.C.; Chojnacky, D.C.; Heath, L.S.; Birdsey, R.A. National-Scale Biomass Estimators for United States Tree Species. *For. Sci.* **2003**, *49*, 12–35. [CrossRef]
40. Domke, G.; Woodall, C.W.; Smith, J.E. Accounting for Density Reduction and Structural Loss in Standing Dead Trees: Implications for Forest Biomass and Carbon Stock Estimates in the United States. *Carbon. Balance Manag.* **2011**, *6*, 14. [CrossRef] [PubMed]
41. Woodall, C.W.; Heath, L.S.; Domke, G.M.; Nichols, M.C. *Methods and Equations for Estimating Aboveground Volume, Biomass, and Carbon for Trees in the U.S. Forest Inventory, 2010*; General Technical Report NRS-88; U.S. Department of Agriculture, Forest Service, Northern Research Station: Newtown Square, PA, USA, 2011.
42. Heath, L.S.; Hansen, M.H.; Smith, J.E.; Smith, B.W.; Miles, P.D. Investigation into Calculating Tree Biomass and Carbon in the FIADB Using a Biomass Expansion Factor Approach. In Proceedings of the 2008 Forest Inventory and Analysis Symposium, Park City, UT, USA, 21–23 October 2008; U.S. Department of Agriculture, Forest Service, Rocky Mountain Research Station: Fort Collins, CO, USA, 2009; pp. 1–26.
43. Day, F.P.; Monk, C.D. Vegetation Patterns on a Southern Appalachian Watershed. *Ecology* **1974**, *55*, 1064–1074. [CrossRef]
44. Van Wagner, C.E. The Line Intersect Method in Forest Fuel Sampling. *For. Sci.* **1968**, *14*, 20–26.

45. Krauss, K.W.; Doyle, T.W.; Twilley, R.R.; Smith, T.J.; Whelan, K.R.T.; Sullivan, J.K. Woody Debris in the Mangrove Forests of South Florida. *Biotropica* **2005**, *37*, 9–15. [CrossRef]
46. U.S. Department of Agriculture, Forest Service, Forest Inventory and Analysis Natonal Program; University of Nevada, Las Vegas. *EVALIDator Web-Application Version 2.1.2*; U.S. Department of Agriculture, Forest Service, Northern Research Station: St. Paul, MN, USA, 2023.
47. Rozendaal, D.M.A.; Requena Suarez, D.; De Sy, V.; Avitabile, V.; Carter, S.; Adou Yao, C.Y.; Alvarez-Davila, E.; Anderson-Teixeira, K.; Araujo-Murakami, A.; Arroyo, L.; et al. Aboveground Forest Biomass Varies across Continents, Ecological Zones and Successional Stages: Refined IPCC Default Values for Tropical and Subtropical Forests. *Environ. Res. Lett.* **2022**, *17*, 014047. [CrossRef]
48. Shukla, P.R.; Skea, J.; Calvo Buendia, E.; Masson-Delmotte, V.; Pörtner, H.-O.; Roberts, D.; Zhai, P.; Slade, R.; Connors, S.; van Diemem, R.; et al. *Climate Change and Land: An IPCC Special Report on Climate Change, Desertification, Land Degradation, Sustainable Land Management, Food Security, and Greenhouse Gas Fluxes in Terrestrial Ecosystems*; Cambridge University Press: Cambridge, MA, USA, 2019; ISBN 9781009157988.
49. Hoover, C.M.; Smith, J.E. Current Aboveground Live Tree Carbon Stocks and Annual Net Change in Forests of Conterminous United States. *Carbon. Balance Manag.* **2021**, *16*, 17. [CrossRef]
50. Conner, W.H.; Inabinette, L.W. Identification of Salt Tolerant Baldcypress (*Taxodium distichum* (L.) Rich) for Planting in Coastal Areas. *New For.* **2005**, *29*, 305–312. [CrossRef]
51. Allen, J.; Pezeshki, S.R.; Chambers, J.L. Interaction of Flooding and Salinity Stress on Baldcypress (*Taxodium distichum*). *Tree Physiol.* **1996**, *16*, 307–313. [CrossRef]
52. Lininger, K.B.; Wohl, E.; Sutfin, N.A.; Rose, J.R. Floodplain Downed Wood Volumes: A Comparison across Three Biomes. *Earth Surf. Process Landf.* **2017**, *42*, 1248–1261. [CrossRef]
53. Woldendorp, G.; Keenan, R.J.; Barry, S.; Spencer, R.D. Analysis of Sampling Methods for Coarse Woody Debris. *For. Ecol. Manag.* **2004**, *198*, 133–148. [CrossRef]